Int. J. Electrochem. Sci., 5 **(2010)** 931 - 943

International Journal of ELECTROCHEMICAL SCIENCE
www.electrochemsci.org

Characterization and Electrocatalytic Activity of Carbon-supported Polypyrrole-Cobalt-Platinum Compounds

W. Martínez M., T. Toledano Thompson, Mascha A. Smit[*]

Centro de Investigación Científica de Yucatán (CICY), Calle 43 No. 130,
Col. Chuburná de Hidalgo, 97200, Mérida, Yucatán, México
[*]E-Mail: mascha@cicy.mx

Received: 10 June 2010 / *Accepted:* 29 June 2010 / *Published:* 15 July 2010

In this paper we report on the physical and electrochemical characterization of carbon-supported materials based on polypyrrole, cobalt and platinum as electrocatalysts for the oxygen reduction reaction (ORR) in PEM fuel cells. Polypyrrole was polymerized onto carbon black (thermally treated at 450°C), and modified with cobalt and/or platinum salts, to obtain carbon-polypyrrole-cobalt, carbon-polypyrrole-platinum and carbon-polypyrrole-cobalt-platinum composites. For comparison, results for unmodified polypyrrole are also reported. It was shown by XRD that the metal-containing materials contain metallic particles within the amorphous polymer samples. The morphology of the composite materials is similar to the carbon support. The platinum-containing materials contain 7% in weight of this element, cobalt-treated materials have 4% in weight of cobalt, and those treated with both salts shows 4% in weight of both metals. Thermal stability was confirmed up to temperatures above 200 °C. It was shown that all materials have electrocatalytic activity for the oxygen reduction reaction (ORR), with the carbon-polypyrrole-platinum compound (C-Ppy-Pt) showing ORR occurring at highest potentials (+0.80 V), due to the presence of platinum. Electrochemical stability was confirmed for the ORR in acid medium. The composite materials were applied as PEMFC cathode catalyst, showing best fuel cell performance for C-Ppy-Pt.

Keywords: electrocatalyst, oxygen reduction reaction, fuel cells, non-platinum catalyst, polypyrrole, X-ray diffraction.

1. INTRODUCTION

Fuel cells directly convert the reactants´ chemical energy into electrical energy with high efficiency, high power density, and good environmental compatibility [1-3]. This explains the increasing attention for fuel cell development, specifically for the polymer electrolyte membrane fuel

cell (PEMFC), to be applied as power sources for vehicles and portable electronic devices [1–3]. Reliability, cost and durability are important considerations for successful commercialization.

The conventional catalysts for PEM fuel cells are platinum-based carbon-supported nanoparticles, which may include other metals such as ruthenium [4-8], for both oxidation of the fuel and reduction of the oxygen at the fuel-cell electrodes. Though platinum-based catalyst shows the lowest overpotential and the highest stability among the metal catalysts, it is an expensive noble metal with low abundance. Reducing the amount of platinum catalyst in hydrogen-air fuel cells, particularly in proton exchange membrane fuel cells (PEMFC´s), has long been an industry goal. Hence, the search for efficient, durable and inexpensive catalysts as alternatives to Pt and Pt-based materials [9-11]. Although ideally the Pt catalyst should be replaced at both fuel-cell electrodes, the substitution of the cathode catalyst for oxygen reduction reaction (ORR) with a non-precious material is likely to result in significantly greater reduction of the Pt needed for fuel cells [12-13].

Recently, cobalt was confirmed as an effective promoter for improving the catalytic activity of mixed oxides catalysts, pyrolized cobalt and cobalt porphyrins [9,10,13-18]. These last materials are potential candidates for oxygen reduction reaction catalysts due to presence the of metal-nitrogen bond [12,16,17]. Oxygen reduction reaction mechanistic studies in the literature have yielded a number of possible active moieties, including Me–N_x centers, graphitized carbon, and transition metal particles. While the activity of the graphitic phases and transition metal particles is debated in the literature, there is a general consensus that a central transition metal atom, such as cobalt, bonded to nitrogen in at least one coordination, does play a role in the electrochemical reduction of oxygen [13,14]. However, durability and cyclic stability have become main drawbacks of metal/porphyrins under practical fuel-cell operating conditions.

Materials based on intrinsically electroconductive polymers (conjugated heterocyclic polymers), such as polypyrrole, polyaniline or polythiophene, on its own, with different dopants, or modified with noble metals, have been shown to have electrocatalytic activity for some specific reactions [14, 18-28], including the ORR.

Recently we have reported on the electrocatalytic activity for the ORR of different conducting polymers supported on carbon black and modified with either cobalt or nickel, [29-31]. Carbon-supported polypyrrole treated with cobalt salt (C-Ppy-Co) [30] was shown to have reasonable electrocatalytic activity, though in a low potential range: The actictivy of these materials is assumed to be related to the creation of active Co-N sites [13-14]. In this paper, the performance of the C-Ppy-Co composite is compared to two novels materials: carbon-supported polypyrrole modified with platinum (C-Ppy-Pt) and with cobalt and platinum (C-Ppy-Co-Pt).

2. EXPERIMENTAL

2.1. *Synthesis of the cathode composite*

Carbon black was treated thermally at 450 ^{o}C during 30 minutes, with the purpose to eliminate sulphur traces and enhanced the electrocatalytic activity [32-33]. The synthesis of the materials: carbon

black-polypyrrole-cobalt (C-Ppy-Co); carbon black-polypyrrole-cobalt-platinum (C-Ppy-Co-Pt); carbon black-polypyrrole-platinum (C-Ppy-Pt) were performed based on previously reported procedure [14,29-31]. First the precursor carbon black-polypyrrole C-Ppy was prepared [29]. Then 4.5 g of this material was mixed with 100 ml of distilled water in a three-necked round-bottom flask, stirring for 10 minutes and heated under reflux to 80 ºC. For the case of C-Ppy-Co, 25 ml of 0.3 M $Co(NO_3)_2 \cdot 6H_2O$ was added; for C-Ppy-Co-Pt, a solution of 1.23 g of $Co(NO_3)_2 \cdot 6H_2O$ and 0.50 g of $Pt(NH_3)_4 \cdot (NO_3)_2$ in 50 ml distilled water was added; in the case of C-Ppy-Pt, 25 ml of 0.05 M of Pt $(NH_3)_4 \cdot (NO_3)_2$ was used. In each case, the obtained mixture was vigorously stirred for 30 minutes at 80 °C, followed by the addition of the reducing agent at 20 ml/min (5.23 g $NaBH_4$ and 0.37 g NaOH in 500 ml distilled water (pH 11.4). The catalysts were filtered and washed repeatedly with distilled water (at 50ºC) until the pH of the filtrate reached 7.0 and dried in air at 100 ºC during 24 hrs.

2.2. Preparation of electrodes

Cathode catalyst ink was prepared mixing the prepared composite materials with distilled water to a ratio of 1:10 by weight and with Nafion® solution (5% 1100 Nafion®; Fluka Corporation) to a 1:1 volumetric ratio. The dispersion was ultrasonically mixed for 5 minutes, while being placed in ice to prevent overheating and minimize evaporation of solvents.

The anode ink was prepared by mixing the anode catalyst (PtRu, 20wt% Pt, 10 wt% Ru/VXC72; Electrochem) using the same methodology and proportions as for the cathode ink. Using a micropipette, 2 µl of the cathode catalyst ink was deposited on a rotating disk electrode with a surface area of 0.071 cm^2. Assuming the catalyst ink to be homogeneous, the dry content of amount of catalyst deposited on the electrode was 47 µg.

2.3. Preparation of MEA

To prepare the gas diffusion layers for anode and cathode, 28 µl of the corresponding catalyst ink was applied to 1 cm^2 of teflon-treated carbon paper (Toray), using a camel hair brush. Assuming the catalyst ink to be homogeneous, the dry content of amount of catalyst deposited on the electrode was 0.66 mg. The MEA was fabricated by hotpressing the electrodes with previously pretreated and activated Nafion 115 at 100 ^oC at 1200 $kgcm^{-2}$ for 5 minutes.

2.4. Characterization

Thermogravimetric analysis (TGA) was carried out in nitrogen atmosphere at a scan rate of 10^oC/min using a Perkin Elmer TGA7.

X-ray diffraction (XRD) was performed on a Siemens D5000 with Cu k□ radiation (Bragg-Bentano, 10s at 0.02° steps).

The morphological and compositional characterization was performed by Scanning Electron Microscopy (SEM) on a JEOL JSM-6360 LV with an INCA Energy 200 microprobe.

Fourier-transform infrared (FT-IR) spectra were obtained by using a Perkin Elmer Spectrum GX. The tests were performed between 2000 and 650 cm^{-1}, with a resolution of 4 cm^{-1}, a scan rate of 0.63 $(cm\ s)^{-1}$, and 15 sweeps per sample.

2.5. Electrochemical characterization

A three-electrode electrochemical cell was used with a graphite counter electrode and a saturated calomel electrode (SCE). Either a stationary or a rotating disk electrode was used as working electrode, depending on the specific test. An Autolab PGSTAT302N potentiostat was used.

Cyclic voltammetry was carried out in 0.5 M H_2SO_4 at room temperature at a scan rate of 20 mV/s. Cathodic potentiodynamic curves were obtained at a scan rate of 1 mV/s, using a RDE at 0, 200, 400, 600, 800 and 1800 rpm. Curves were started from the open circuit potential, E_{oc}, down to the potential at which the current density reached is maximum on the ORR peak, as determined from cyclic voltammetry tests for each sample. Potentiostatic tests were carried out using a stationary electrode and applying the maximum potential of the ORR peak as determined from cyclic voltammetry. All potentials are reported vs NHE.

2.6. Fuel cell testing

The fuel cell hardware consisted of a 1 cm^2 cell with graphite endplates with serpentine gas channels. After activation of the MEA, fuel cell tests were performed using a Scribner Fuel Cell Test Station 850C and a Gill AC potentiostat. Flow rates of hydrogen and oxygen were 5 ml s^{-1} and 9 ml s^{-1}, respectively. I-V curves were measured at room temperature. Ohmic resistance was determined by electrochemical impedance.

3. RESULTS AND DISCUSSION

3.1. *Morphology and elemental analysis*

Figure 1 shows SEM images for thermally treated carbon black (fig. 1.a), C-Ppy (fig. 1.b) and C-Ppy-Co-Pt (fig. 1.c). As for previously reported materials [29-31], the morphology for the polymer-containing samples is very similar to the carbon black morphology, however, the structure appears to be less porous, due to the deposited polymer. Small grains with diameters between 0.07 and 0.12 μm are observed for all the materials.

Table 1 shows the chemical composition as obtained by EDAX. As expected, the main element is carbon, with quantities varying from 82 to 94%wt coinciding with the estimated values (see experimental section). Also significant quantities of oxygen are found for all samples. The thermal treatment resulted in an increased oxygen quantity of 8%wt (compared to 6%wt) for carbon black, assumed to be present as superficial oxygen in the form of oxygen functional groups [32].

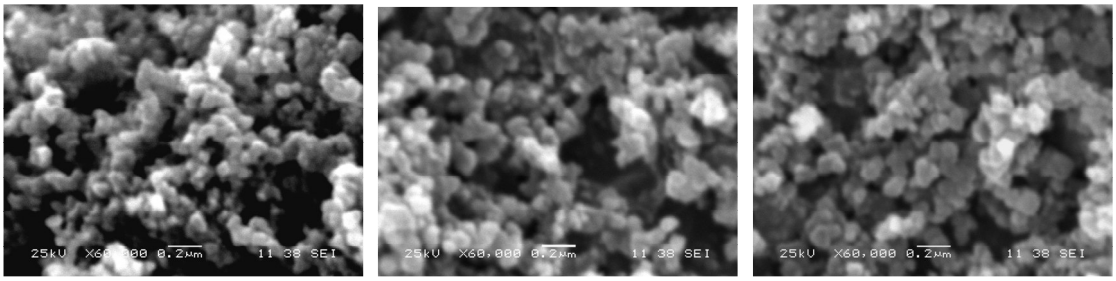

Figure 1. Micrographs obtained by SEM for a) thermally treated carbon black; b) C-Ppy and c) C-Ppy-Co-Pt.

The amount of oxygen increases for metal-polymer-containing samples (compared to carbon black), which is in agreement with FTIR results, corresponding to CO bonds, as well as metal oxides or metal hydroxides.

For C-Ppy-Co, cobalt is present in 4%wt, less than expected based on initial reactant ratios. The same is observed for platinum present in the C-Ppy-Pt sample (7%wt) and Co and Pt, both present in 4%wt in C-Ppy-Co-Pt. It was not possible to detect the nitrogen content, due to its overlap with the large carbon peaks.

Table 1. Chemical composition in weight percent as obtained by EDAX.

	Weight (%)				
Sample	**C**	**O**	**Pt**	**Co**	**Total**
Carbon black	94	6	--	--	100
Carbon black T.T.	92	8	--	--	100
C-Ppy	90	10	--	--	100
C-Ppy-Co	86	10	--	4	100
C-Ppy-Co-Pt	82	10	4	4	100
C-Ppy-Pt	82	11	7	--	100

3.2. Thermogravic analysis

The results obtained from TGA are shown in figure 2. Carbon black was included as a reference. It can be seen that the thermal treatment at 450^{o}C increases the thermal stability of the carbon at high temperatures. C-Ppy, begins to decompose at around 450^{o}C, showing slow mass loss, possibly related to carbon degradation. C-Ppy-Pt and C-Ppy-Co-Pt show nearly identical behaviour, both materials begin to lose mass at 350^{o}C, with a slow decomposition at higher temperatures. C-Ppy-Co begins to decompose at 225^{o}C, after this it has a faster initial mass loss as compared to C-Ppy-Co-Pt or C-Ppy-Pt samples.

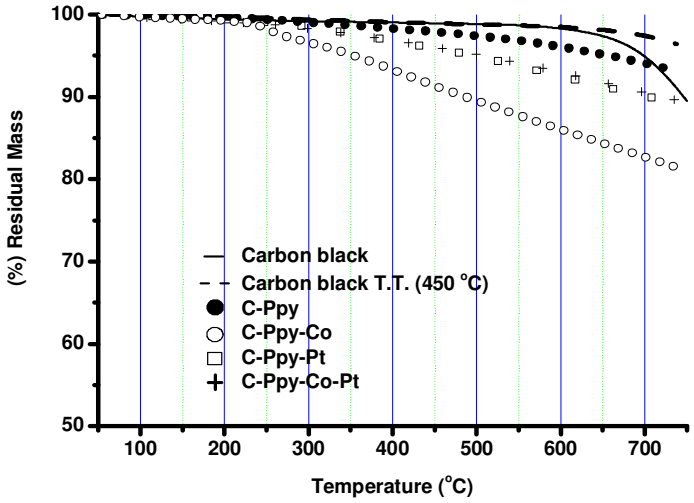

Figure 2. TGA curves obtained in nitrogen atmosphere.

However, C-Ppy-Co, C-Ppy-Pt and C-Ppy-Co-Pt do not show the rapid decomposition at high temperature (above 650°C) as observed for untreated carbon black, indicating improved thermal stability. The decomposition at lower temperatures of these materials is assumed to be related to the degradation of metal compounds, such as oxides [32]. These materials are thermally stable in the PEMFC´s operation temperature range (60 - 100°C).

3.3. FTIR

The FTIR spectra obtained for the C-Ppy-Pt, C-Ppy-Co-Pt, C-Ppy-Co, and C-Ppy are shown in figure 3. It can be seen that for all samples, most of the bands correspond to carbon black, specifically bands in the ranges of: 1635-1631 cm^{-1}, 1390-1382 cm^{-1}, 1124-1116 cm^{-1}, 1029-1018 cm^{-1}, and 669 - 667 cm^{-1} [35,36].

For C-Ppy (fig. 3.a), there is a small band at 747 cm^{-1} related to C-H vibrations [37,38]. A band near 1220 cm^{-1} is related to C-N vibration. The strong peak seen at 1602 cm^{-1} corresponds to a C=O bond and C-N, C-O stretching vibrations can be found at 1132 cm^{-1}.

It can be observed that for C-Ppy-Co, C-Ppy-Co-Pt and C-Ppy-Pt, (figs. 3.b-d) the spectra are very similar in shape as for the C-Ppy precursor, but with different intensity for a number of bands. These intensity changes are most evident at 1635-1602 cm^{-1} (related to C=C and C=O bond), at 1382-1390 cm^{-1} (CO), and at 1116-1124 cm^{-1} and 1027-1018 cm^{-1} (related to C-N bonds). There is no indication for a change of the polypyrrole structure due to the modification with Pt or Co.

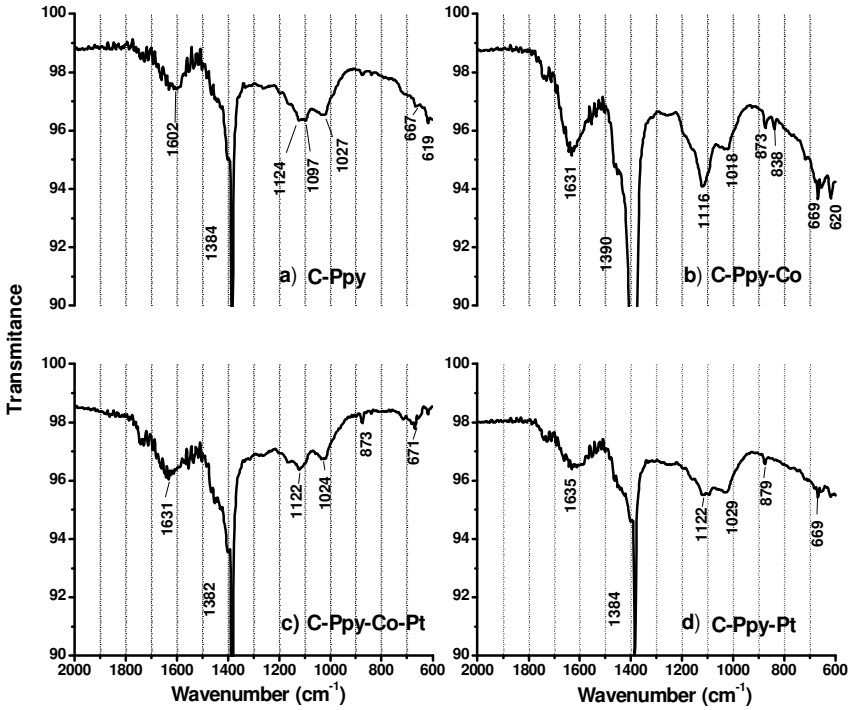

Figure 3. FTIR spectra obtained for: a) C-Ppy; b) C-Ppy-Co; c) C-Ppy-Co-Pt and d) C-Ppy-Pt.

3.4. XRD

X-ray diffraction was performed on all samples and results are shown in figure 4. It was found that Ppy was completely amorphous, while C-Ppy-Pt clearly showed the presence of metallic platinum. C-Ppy-Co-Pt did not show metallic platinum, however, the presence of bimetallic cobalt-platinum compounds (PtCo or $PtCo_3$) is indicated by a broad peak at 40°, compounds which been reported to show electrocatalytic activity for oxygen reduction [39-41].

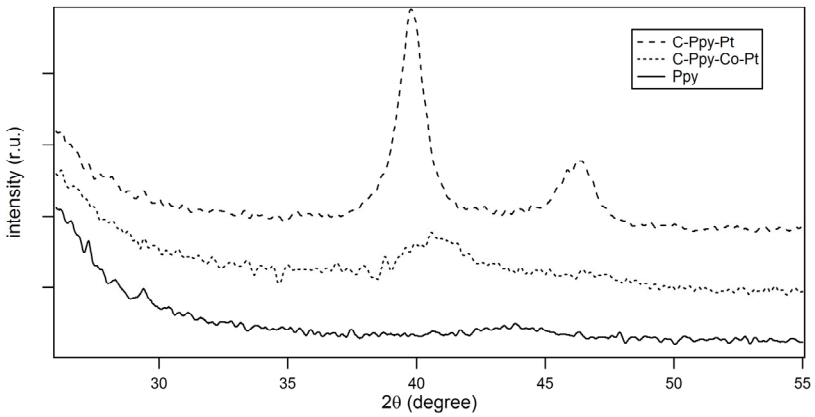

Figure 4. X-ray diffraction spectra obtained for Ppy, C-Ppy-Pt and C-Ppy-Co-Pt.

3.5. Electrochemical characterization

The activity of these materials for the oxygen reduction reaction (ORR) was determined by cyclic voltammetry, see figure 5. The continuous lines correspond to an electrolyte saturated with oxygen and the dashed lines to oxygen-free atmosphere (under nitrogen). In oxygen-free electrolyte, curves show typical oxidation and reduction currents due to changes in the oxidation state of polypyrrole [26,28]. For example, C-Ppy shows polymer reduction and oxidation around 400 mV, while for C-Ppy-Co this occurs at around 500 mV. C-Ppy-Co-Pt and C-Ppy-Pt curves are very similar in shape, although the last sample shows higher current densities, indicating higher electrocatalytic activity.

In order to be able to compare the ORR electrocatalytic activity for the different samples, the difference between the maximum current density for each ORR peak and the current density in its base were determined and related to the maximum anodic current density (as a measure for the amount of polymer). The current difference between maximum and base in the ORR peak was highest for C-Ppy-Pt (-3.30 mA/cm^2), followed closely by C-Ppy-Co-Pt (-1.72 mA/cm^2), C-Ppy-Co (-1.19 mA/cm^2), and C-Ppy (0.70 mA/cm^2).

The potentials at which oxygen reduction takes place (at maximum current density for ORR from figure 5) were determined and are also listed in table 2. It can be seen that highest potential is obtained in the order of C-Ppy-Co-Pt (0.80 V) > C-Ppy-Pt (0.75 V) > C-Ppy-Co (0.31 V).

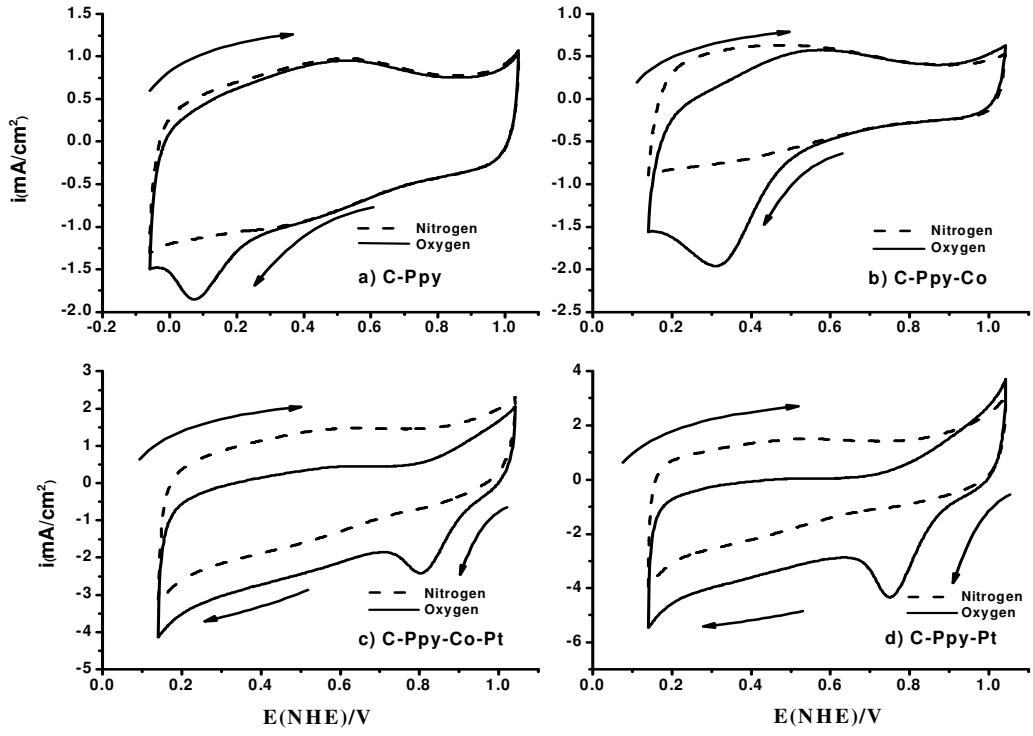

Figure 5. Cyclic voltammetry for: a) C-Ppy; b) C-Ppy-Co; c) C-Ppy-Pt; d) C-Ppy-Co-Pt, carried out at room temperature in 0.5 M H_2SO_4 at 20 mV/s.

In order to determine the stability of the materials in the acid environment during oxygen reduction, potentiostatic experiments were carried out under oxygen (see figure 6), applying for each sample the potential at which the maximum current density for ORR was observed from cyclic voltammetry (see figure 4 and table 2). All samples show a small, but continuous decrease in current density during the 2 days of experiment, possibly related to bonding of cobalt, and/or platinum atoms to the polymeric chain, with metallic cobalt transforming into Co(II), with the formation of a coordination bond between Co(II) and N or O, improving stability for the composite [14].

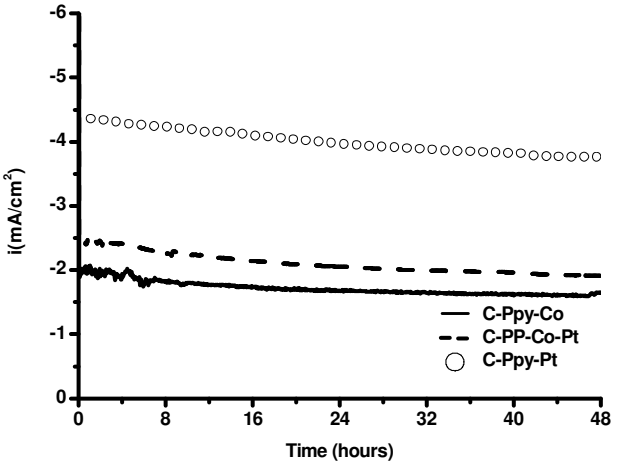

Figure 6. Cronoamperometric curves for C-Ppy-Co, C-Ppy-Co-Pt, and C-Ppy-Pt in 0.5 M H_2SO_4 under oxygen.

In figure 7 the curves for electrochemical reduction of molecular oxygen in a half cell are shown for C-Ppy-Co, C-Ppy-Co-Pt and C-Ppy-Pt in 0.5 H_2SO_4, obtained at different rotation speeds, using a rotating disk electrode (RDE) and a scan rate of 1 mV/s. The experiments were carried out starting from the open circuit potential (E_{oc}) of each electrode until reaching the potential where highest current density on the ORR peak was obtained.

At overpotentials above 0.43 V for C-Ppy-Co, 0.89 V for C-Ppy-Co-Pt and 0.82 V for C-Ppy-Pt, the reaction rates are determined by electron transfer. At low overpotentials, below 0.35 V for C-Ppy-Co, 0.82 V for C-Ppy-Co-Pt and 0.77 V for C-Ppy-Pt, the process is controlled by oxygen diffusion. Mixed control is observed from 0.35 to 0.43 V for C-Ppy-Co, 0.82 to 0.89 V for C-Ppy-Co-Pt and 0.77 to 0.82 V for C-Ppy-Pt. Kinetic parameters were obtained from this last interval for each sample and are presented in table 2 [4,6,10].

C-Ppy-Co has the lowest open circuit potential with 0.76 V vs NHE and C-Ppy-Co-Pt and C-Ppy-Pt have the same value: 0.98 V. The transfer coefficient values (α) are very similar for all samples. Tafel slope values of 110 V/dec for C-Ppy-Co-Pt and C-Ppy-Co indicate that the first electron transfer is the decisive step in the global ORR [4,5], and posibly for C-Ppy-Co-Pt also, having a slightly lower value (105 mV/dec). C-Ppy-Pt has the highest exchange current density (i_o) with 6.3 x 10^{-2} mA/cm^2,

followed by C-Ppy-Co-Pt with 5.1 x 10^{-2} mA/cm^2 and C-Ppy-Co with 4.2 x 10^{-2} mA/cm^2, results which agrees with those seen in figure 5.

It can be seen from table 2 that the addition of platinum and/or cobalt, not only changes the potential range for ORR to more positive values, but also the kinetic parameters, Tafel slope and exchanged current density [29-31]. Based on these data, of the materials studied, C-Ppy-Co-Pt and C-Ppy-Pt show good performance for ORR. Best performance for RRO, was reported previously for cobalt-modified polypyrrole (supported on untreated carbon black), which had the most positive potential (325 mV), followed by unmodified C-Ppy (93 mV), although with lower exchange current densities, possibly due to the thermal treatment of the carbon black [32,33].

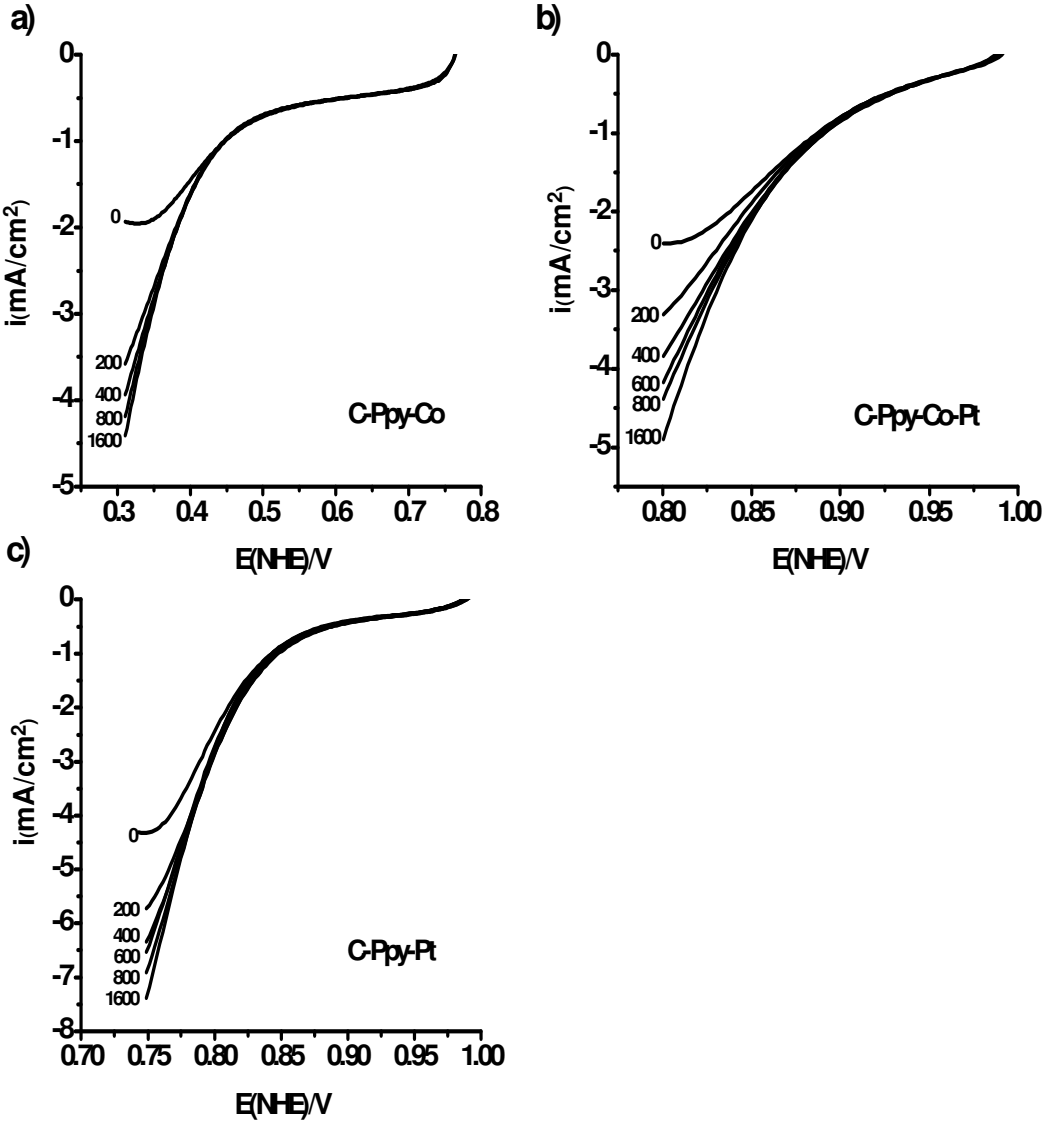

Figure 7. Results from rotating disk voltammetry at 1 mV/s in 0.5 M H_2SO_4 saturated with oxygen for: a) C-Ppy-Co b) C-Ppy-Co-Pt and c) C-Ppy-Pt.

Table 2. Electrokinetic parameters obtained from RDE experiments.

Electrode	E_{oc} (V/NHE)	$-b$ (V/dec)	α	i_o (A/cm^2)	E (V) at $i_{max\ ORR}$
C-Ppy-Co	0.76	110	0.60	4.2 x 10^{-5}	0.31
C-Ppy-Co-Pt	0.98	105	0.50	5.1x 10^{-5}	0.80
C-Ppy-Pt	0.98	110	0.55	6.3 x 10^{-5}	0.75

3.6. Fuel cell performance

Polarization curves and resulting power densities plots obtained from fuel cell tests performed at room temperature are shown in figure 8.a and .b respectively. The cathode catalyst is one of the newly synthesized composites, while anodes contain Pt/Ru catalyst.

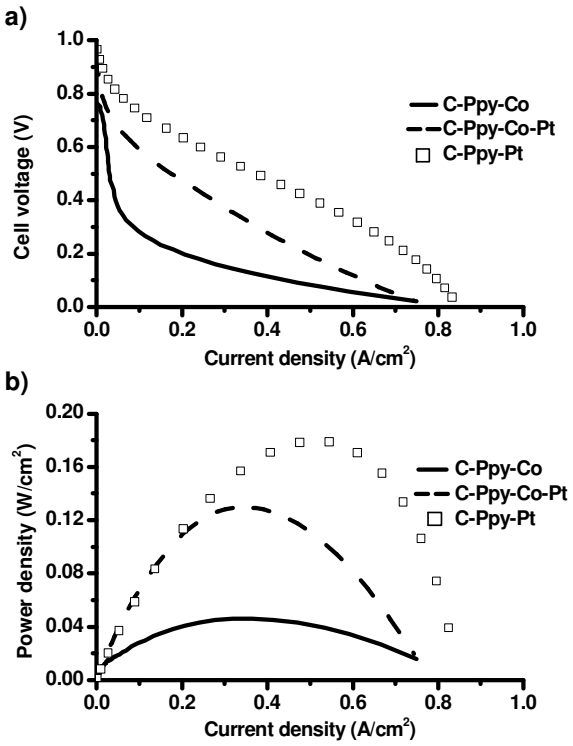

Figure 8. Fuel cell performance plots for MEA's with C-Ppy-Co, C-Ppy-Co-Pt and C-Ppy-Pt cathode catalyst: a) Polarization curves; b) Power densities.

Highest current densities are obtained for C-Ppy-Pt catalysts. The catalyst generates 0.52 A/cm^2 at 0.39 V and its maximum power density reached was 0.20 W/cm^2. The second best performance was obtained by C-Ppy-Co-Pt, generating 0.35 A/cm^2 at 0.32 V and a maximum power density of 0.11 W/cm^2. C-Ppy-Co produces 0.36 A/cm^2 at 0.127 V, reaching 0.04572 W/cm^2. The open

circuits voltages are as follows: C-Ppy-Pt (0.97 V) > C-Ppy-Co-Pt (0.90 V) > C-Ppy-Co (0.75 V) (see table 3).

Bashyam [14] reported on a composite similar to the C-Ppy-Co catalyst synthesized here, tested in a PEM fuel cell at a higher operating temperature (80^{o}C) and higher absolute oxygen pressure (2.8 atm), and obtained 0.2 A/cm^2 at 0.5 V with maximum power density of 0.14 W/cm^2. Cobalt-polypyrrole supported on multiwalled carbon nanotube composite [13] was reported to generate 0.15 A/cm^2 at 0.5 V at 90^{o}C. C-Ppy-Pt compares favorably to other precious metal-based materials, such as Pd-Co-Au alloy (0.18 A/cm^2 at 0.50V, 60^{o}C, 1.5 atm oxygen back pressure) and Pd-Ti alloy (0.1 A/cm^2 at 0.50 V, 60^{o}C and 0.2mg/cm^2) [42].

4. CONCLUSIONS

The properties and electrocatalytic activity of candidate cathode catalyst for PEM fuel cells, based on carbon-supported polypyrrole modified with cobalt and/or platinum were studied.

The morphology for all samples was found to be similar, and reflects tha carbon suppor morphology. It was shown that metallic particles (Pt) and bimetallic particles (PtCo or Pt Co_3) are present in th Pt and Co-Pt containing samples. The thermal and electrochemical stability of the samples was confirmed for simulated fuel cell conditions. Electrochemical tests, such as cyclic voltammetry, showed that in the potential range studied, all materials have electrocatalytic activity for the ORR. The addition of platinum to C-Ppy results in more positive potentials for ORR than for the addition of Co only. In the case of the combined addition of both metals (C-Ppy-Co-Pt) results are very similar to the catalyst containing Pt only (C-Ppy-Pt), which has almost double the amount of Pt. The potential at which ORR occurs was determined to be highest for C-Ppy-Pt, followed by C-Ppy-Co-Pt, C-Ppy-Co and at last C-Ppy. Kinetic parameters, calculated from lineal voltammetry using RDE, show that C-Ppy-Co-Pt has highest exchange current densities. It is assumed that the presence of the metallic particles play in important role in the high electrocatalytic activity of these samples. Based on fuel cell tests, however, the best composite is the C-Ppy-Pt, showing higher open circuit potential and higher current densities.

ACKNOWLEDGEMENTS
We appreciate the financial support given by Conacyt through the projects 47066-Y and 58636. We also thank Wilberth Herrera K. and Enrique Escobedo Hernández for their help in TGA, FTIR and fuel cell tests, and Daniel Aguilar Treviño (Cinvestav-Mérida) for help in XRD.

References

1. W. McDowall and M. Eames, *Int. J. Hydrogen Energy*, 32 (2007) 4611-4626.
2. H. Wendt, *Quim. Nova*, 28 (2005) 1066-1075.
3. M.Z. Jacobson, W.G. Collela and D.M. Gonden, *Science*, 308 (2005) 1901-1905.
4. R.G. González-Huerta, M.A. Leyva and O. Solorza-Feria, *Rev. Soc. Quím. Méx*. 48 (2004) 1-6.

5. D. Cao, A. Wieckowski, J. Inukai and N. Alonso-Vante, *J. Electrochem. Soc.*, 153 (2006) A869-A874.
6. N. Alonso-Vante, H. Tributsch and O. Solorza-Feria, *Electrochim. Acta*, 40 (1995) 567-576.
7. Y. Zhang, C. Wang, N. Wan and Z. Mao, *Int. J. Hydrogen Energy*, 32 (2007) 400-404.
8. B. Krishnamurthy and S. Deepalochani, *Int. J. Electrochem. Sci.,* 4 (2009) 386 – 395.
9. S. Pylypenko, S. Mukherjee, T.S. Olson and P. Atanassov, *Electrochim. Acta*, 53 (2008) 7875-7883.
10. K. Yamamoto and D. Taneichi, *J. Inorg. Organomet. Pol.,* 9 (1999) 231-243.
11. H.L. Hellman, R. Van den Hoed, *Int. J. Hydrogen Energy*, 32 (2007) 305-315.
12. H.P. Chang, C.L. Chou, Y.S. Chen, T. Hou and B.J. Weng, *Int. J. Hydrogen Energy*, 32 (2007) 316-322.
13. M.R. Arava Leela, R. Natarajan and R. Sundara, *Carbon*, 46 (2008) 2-11.
14. R. Bashyam, and P. Zelenay, *Nature Lett*., 443 (2006) 63-65.
15. R. Atanososky, *Report VIIC9*, US DOE (2005).
16. B. Wang, *J. Power Sources*, 152 (2005) 1-15.
17. G. Faubert, G. Lalande, R. Cote, D. Guat, J.P. Dodelet, L.T. Weng, P. Bertrand, and G. Denes, *Electrochim. Acta*, 41 (1996) 1689-1701.
18. Yohannes Kiros, *Int. J. Electrochem. Sci.,* 2 (2007) 285-300.
19. J. Jagur-Grodzinski, *Polym. Adv. Technol.* 18 (2007) 785-799.
20. M.A. Careema, Y. Velmurugu, S. Skaarup and K. West, *J. Power Sources*, 159 (2006) 210-214.
21. R. Naujikas, A. Malinauskas, and F. Ivanauskas, *J. Math. Chem.*, 42 (2007) 1069-1084.
22. V.G. Khomenko, V.Z. Barsukov and A.S. Katashinskii, *Electrochim. Acta*, 50 (2005) 1675-1683.
23. N. Chatterjee and I.N. Basumallick, *J. Power Sources*, 63 (1996) 271-273.
24. K. Yamamoto and D. Taneichi, *J. Inorg. Organomet. Pol.*, 9 (1999) 231-243.
25. N. Alonso-Vante, S. Cattarin and M. Musiani, *J. Electroanal. Chem.*, 481 (2000) 200-207.
26. R.N. Singh, B. Lal and M. Malviya, *Electrochim. Acta*, 49 (2004) 4605-4612.
27. E.K.W. Lai, P.D. Beattie and S. Holdcroft, *Synth. Met.*, 84 (1997) 87-88.
28. H.N. Cong, K. El Abbassi, J.L. Gautier and P. Chartier, *Electrochim. Acta*, 50 (2005) 1369-1376.
29. W. Martínez-Millan, T. Toledano-Thompson, L.G. Arriaga and M.A. Smit, *Int. J. Hydrogen Energy*, 34 (2009) 694-702.
30. W. Martínez-Millan and M.A. Smit, *J. Appl. Pol. Sci.*, 112 (2009) 2959-2967.
31. R. Sulub, W. Martínez-Millan and M.A. Smit, *Int. J. Electrochem. Sci.*, 4 (2009) 1015-1027.
32. C.W.B. Bezerra, L. Zhang, H. Liu, K. Lee, A.L.B. Marques, E.P. Marques, H. Wang and J. Zhang, *J. Power Sources*, 173 (2007) 891-908.
33. Y. Xingwen, Y. Siyu, *J. Power Sources*, 172 (2007) 133-144.
34. K.H. Kim, H.J. Kim, K.Y. Lee, J.H. Jang, S.Y. Lee, E. Cho, I.H. Oh, and T.H. Lim, *Int. J. Hydrogen Energy*, 33 (2008) 2783-2789.
35. G.C. Panda, S.K. Das, T.S. Bandopadhyay and A.K. Guha, *Colloids and Surfaces*, 57 (2007) 135-142.
36. M. Trchova, I. Sedeonkova and J. Stejskal, *Synth. Met.*, 154 (2005) 1-4.
37. E. Ando, S. Onodera, M. Iino and O. Ito, *Carbon*, 39 (2001) 101-108.
38. D.H. Park, B.H. Kim, M.G. Jang, K.Y. Bae and J. Joo, *Appl. Phys. Lett*., 86 (2005) 113-116.
39. H. Schulenburg, E. Müller, G. Khelashvili, T. Roser, H. Bünnemann, A. Wokaun and G.G. Scherer, *J. Phys. Chem. C*, 113 (2009) 4069-4077.
40. J.S. Sang, H.I. Joha, T.K. Hyun and S.H. Moon, *J. Power Sources*, 163 (2006) 403-408.
41. M.K. Jeon, Y. Zhang and P.J. McGinn, *Electrochim. Acta*, (2010) in press.
42. J.L. Fernandez, V. Raghuveer, A. Manthiram and A.J. Bard, *J. Am. Chem. Soc.*, 127 (2005) 13100-13101.